

Two-Dimensional Ordering of Bacteriorhodopsins in a Lipid Bilayer and Effects Caused by Repulsive Core between Lipid Molecules on Lateral Depletion Interaction: A Study based on a Thermodynamic Perturbation Theory

Keiju Suda^a, Ayumi Suematsu^b, Ryo Akiyama^a

^a*Department of Chemistry, Graduate School of Science, Kyushu University, Motoooka 744, Nishi-ku, Fukuoka-shi, 819-0395, Fukuoka, Japan*

^b*Faculty of Science and Engineering, Kyushu Sangyo University, Matsukadai 2-31, Higashi-ku, Fukuoka-shi, 813-8503, Fukuoka, Japan*

Abstract

Using binary hard disk mixture models, we studied the two-dimensional ordering of bacteriorhodopsins in a lipid bilayer. The phase diagrams were calculated using the thermodynamic perturbation theory. We examined two types of effective interactions to discuss the lateral depletion effects caused by repulsive core interaction between lipid molecules. The results indicate that the core repulsions drastically broaden the coexistence region for the fluid-ordered phase.

1. INTRODUCTION

Bacteriorhodopsin (bR) is a transmembrane protein [1, 2]. The wild-type bRs form trimers, and the trimers construct a two-dimensional ordering structure in the membrane of *Halobacterium salinarum*, which is an archaeobacterium. The hexagonal ordering structure is not infinite, but it has been called a two-dimensional crystal of bR. There is no chemical bond between bRs [3], and the driving force of this ordering is unclear.

Our previous study[4] suggested that the lateral depletion effect[5–26] is dominant in the driving force of ordering. The study focused on the difference between the “crystallization” behaviors of wild-type bR and mutant bR, which construct the ordering structure. Although the mutant monomers

do not construct trimers, they form a crystal[27]. The critical concentrations (CCs) of the mutant bRs for the “crystallization” are much larger than those of the wild-type bRs. According to experiments by M. P. Krebs et al., the ratio CCR(= CC1/CC3) is about 10.2, where CC1 and CC3 are the critical concentrations for the mutant monomers and the wild-type trimers, respectively[28].

In the previous study [4], we calculated the phase diagram using simple theories for two-dimensional binary hard-disk systems. There is a reason for adopting this simple approach. Several researchers have adopted similar approaches in the study of three-dimensional binary hard-sphere systems and reported adequate results[12–25]. Therefore, we applied the ideas to two-dimensional systems. There are some studies on the binary hard-disk system [29–31]. However, the size ratio was far from that for the lipid molecule/bR. In our studies, the size ratio was limited from lipid molecule/bR monomer to lipid molecule/bR trimer[4]. The binary hard-disk system, composed of bR and lipid molecules, was connected with a lipid reservoir. We obtained the free energies for the fluid and ordered phases based on the free volume idea[12, 13] and calculated the phase diagram.

The calculated results indicated that the depletion effect was too weak when the lipid molecules were modeled as an ideal gas, and it differed from the experimental result[4]. On the other hand, we also described the pressure of the reservoir using the two-dimensional scaled particle theory (2D–SPT)[32, 33], taking into account the effects of the repulsive core of the lipid molecule[4]. We calculated the phase diagrams based on the models. The calculated phase diagrams showed that the repulsive core enhanced the depletion effect, and the calculated CCRs virtually agreed with the experimental results [4]. Therefore, we discussed that the depletion effect significantly contributed to the “crystallization”.

The reduced effective second virial coefficients for bRs were also calculated to discuss the depletion effects of the phase diagram calculation in a previous study[4]. We examined two depletion interactions: namely, the Asakura–Oosawa (AO) [5, 6] and the modified Asakura–Oosawa (modified AO) interactions[4]. The core repulsion between lipid molecules is ignored in the AO interaction. On the other hand, taking account of the core repulsion between the lipid molecules, we adopted 2D–SPT in the modified AO theory. As a result, the reduced effective second virial coefficients only for the modified AO interactions showed large negative values. Therefore, the phase diagrams and the reduced effective second virial coefficients were

consistent. However, the phase behaviors of bR of this effective interaction have not been obtained in the previous paper[4].

In the previous simple approach[4], we obtained the phase diagrams without calculating the effective interaction between bRs. We study similar problems of CCR in the present paper, but the phase diagrams are now calculated using a completely different approach. First, we calculated the effective interactions between bR. Next, we calculated the free energies using the thermodynamic perturbation theory[24, 25, 34] with the effective interactions and obtained the phase diagrams. Finally, the phase diagrams gave us CCRs.

2. Model and Theory

We adopted a binary hard-disk model in the present study. The model is the same as that in reference[4]. The lipid bilayer was regarded as a condensed 2D plane space. The lipid molecules, bR monomers, and bR trimers were modeled as small, medium, and large hard disks, respectively. The diameter for the bR trimer σ_{tri} was estimated as 6.2 nm[4, 35]. The diameter for the bR monomer σ_{mono} was estimated as 3.0 nm[4]. The diameter for the lipid molecule σ_{lip} was estimated as 0.5 nm[4, 36]. In addition, the two lipid diameters $\sigma_{\text{lip}} = 0.4$ and 0.6 nm were also examined to remove the arbitrariness for the model.

The system consisted of lipid and bR molecules. The binary hard-disk system was in osmotic equilibrium with a reservoir. Therefore, we obtained the effective interactions between bR molecules and calculated the phase diagrams using the effective one-component system. The effective interactions between bR molecules are explained as follows.

The AO and modified AO potentials[4] were adopted as the effective potential for bRs. The lipid molecules cannot enter the excluded area V_{ex} around the bR molecules in this model. The AO potential ω_{AO} between bRs can be written as

$$\omega_{\text{AO}}(r) = \infty, \quad r < \sigma_{\text{bR}}, \quad (1)$$

$$\omega_{\text{AO}}(r) = -\rho_{\text{lip}}^{\text{res}} k_B T \Delta V_{\text{ex}}(r), \quad r > \sigma_{\text{bR}}, \quad (2)$$

where $\rho_{\text{lip}}^{\text{res}}$ is the number density of lipid molecules in the reservoir, k_B is Boltzmann constant, T is the absolute temperature, ΔV_{ex} is the overlap area of excluded volumes, r is the distance between centers of bRs, and σ_{bR} is the

diameter for bR. ΔV_{ex} is expressed analytically as follows,

$$\begin{aligned} \Delta V_{\text{ex}}(r) &= \frac{1}{2} \sigma_{\text{bR}}^2 (1+q)^2 \arccos \left[\frac{r}{\sigma_{\text{bR}}(1+q)} \right] \\ &\quad - \frac{1}{4} \sigma_{\text{bR}}^2 (1+q)^2 \sin \left[2 \arccos \left[\frac{r}{\sigma_{\text{bR}}(1+q)} \right] \right] \end{aligned} \quad (3)$$

where q is the diameter ratio between the lipid molecule and bR ($\sigma_{\text{lip}}/\sigma_{\text{bR}}$). $\rho_{\text{lip}}^{\text{res}} k_{\text{B}} T$ is regarded as the pressure of ideal gas in the reservoir. Therefore, the AO interaction is the pressure-area work for the two-dimensional ideal gas, and the area is ΔV_{ex} [12].

In the conventional AO theory, the repulsive interactions between depletants are ignored, and the lipid molecules overlap. In other words, the pressure in the reservoir is that of the ideal gas. On the other hand, we replaced the pressure of the ideal gas reservoir with that estimated using the two-dimensional scaled particle theory (2D-SPT)[4, 12], taking account of the repulsive interactions between depletants. Thus, the pressure in the reservoir was expressed as follows:

$$p^{\text{res}} = \frac{\rho_{\text{lip}}^{\text{res}}}{(1 - \eta_{\text{lip}}^{\text{res}})^2} k_{\text{B}} T, \quad (4)$$

where $\eta_{\text{lip}}^{\text{res}}$ is the reservoir's packing fraction of lipid molecules. Here, we call this the modified AO model. The modified AO potential ω_{Mod} , therefore, was written as

$$\omega_{\text{Mod}}(r) = \infty, \quad r < \sigma_{\text{bR}}, \quad (5)$$

$$\omega_{\text{Mod}}(r) = -\frac{\rho_{\text{lip}}^{\text{res}}}{(1 - \eta_{\text{lip}}^{\text{res}})^2} k_{\text{B}} T \Delta V_{\text{ex}}(r), \quad r > \sigma_{\text{bR}}. \quad (6)$$

In this model, there are only two bRs in the lipid condensed system. That is, we assumed a very low bR packing fraction in the system. As the bR packing fraction increases, the lipid packing fraction in the system decreases. Therefore, the effective interaction depends on the bR packing fraction. Here, we adopted an approximation that ω_{Mod} is independent of the bR packing fraction[24, 25].

FIG. 1 shows the effective potentials at $\eta_{\text{lip}}^{\text{res}} = 0.5$. The stability at the contact distance for the modified AO potential is much larger than that

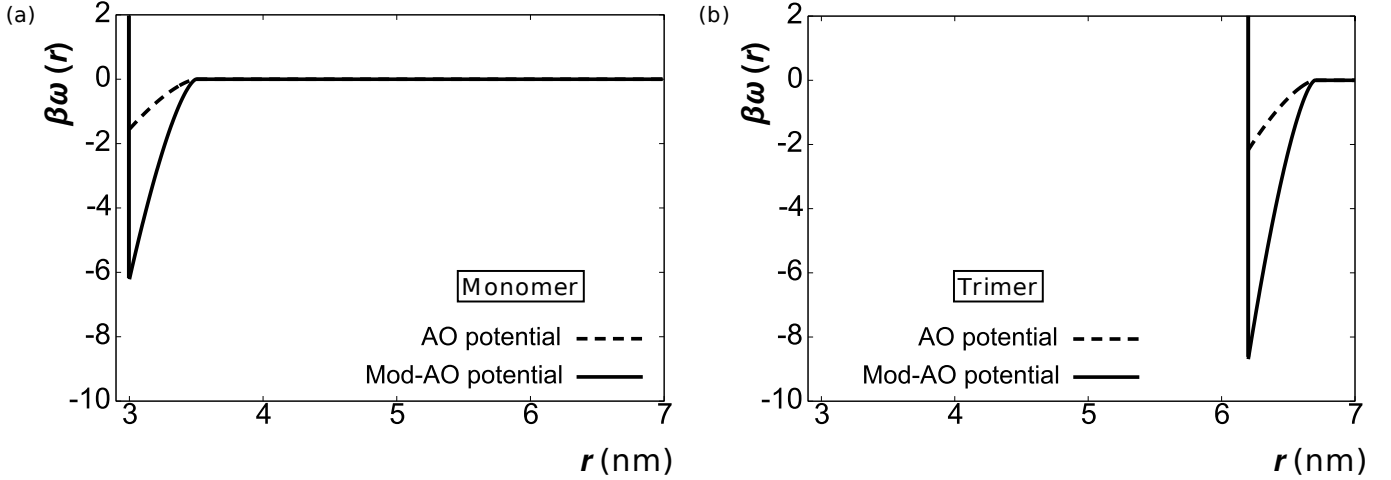


Figure 1: The effective potential between bR monomers (a) and trimers (b) at $\eta_{\text{hip}}^{\text{res}} = 0.5$. The lipid—bR diameter ratios, q_s , are 0.16667 and 0.08065, respectively. The dashed curves show the AO potential. The solid curves show the modified AO potential.

for the AO potential. The ratio is larger than three in the case of the bR monomers (FIG. 1(a)). That is, the effective attraction for the modified AO potential is much stronger than that for the AO potential. In addition, the stability ratio becomes larger as the size ratio q decreases. Thus, the stability ratio becomes larger than four in the case of the trimer (FIG. 1(b)).

Here, we mention the difference between the AO and the modified AO potentials. We prepared the pressure in calculating the quasistatic PV-work to change the excluded volume of bRs for the lipid fluid. In the case of the AO potential, the pressure of the ideal gas was used. On the other hand, we adopted 2D-SPT in the case of the modified AO potential. The latter pressure is higher than the former because of the packing effect of the lipid hard disks. Therefore, the stability of the contact bR dimer for the modified AO potential is much larger than that for the AO potential.

To obtain the phase diagrams, we adopted the thermodynamic perturbation theory. In the perturbation theory, the Helmholtz free energy for the effective one-component system $F(N_{\text{bR}}, V, T)$ was expressed as follows:

$$\frac{\beta F(N_{\text{bR}}, V, T) v_{\text{bR}}}{V} = \frac{\beta F_0(N_{\text{bR}}, V, T) v_{\text{bR}}}{V} + 4\beta\eta_{\text{bR}}^2 \int_0^\infty g_0\left(\frac{r}{\sigma_{\text{bR}}}\right) \omega\left(\frac{r}{\sigma_{\text{bR}}}\right) \frac{r}{\sigma_{\text{bR}}} d\left(\frac{r}{\sigma_{\text{bR}}}\right), \quad (7)$$

where V is the area of the system, v_{bR} is the area of one bR, F_0 is the

Helmholtz free energy for the pure bR system, η_{bR} is the packing fraction of the bRs, $\omega(\frac{r}{\sigma_{\text{bR}}})$ is the effective potential between bRs, and $g_0(\frac{r}{\sigma_{\text{bR}}})$ is the radial distribution function for the pure bR system scaled by σ_{bR} .

In the previous paragraph, the calculation of the perturbation part needed the radial distribution function. The radial distribution functions were obtained using the event chain Monte Carlo simulation[37]. The simulation box has 128^2 hard disks, and the sampling was carried out over 1.2×10^{11} steps after equilibration. The radial distribution functions were calculated within the ranging from $\eta_{\text{bR}} = 0.001$ to $\eta_{\text{bR}} = 0.905$ in the interval of $\eta_{\text{bR}} = 0.001$. The AO or the modified AO potential were substituted in $\omega(\frac{r}{\sigma_{\text{bR}}})$.

F_0 was obtained by thermodynamics as follows:

$$\frac{\beta F_0 v_{\text{bR}}}{V} = \beta \eta_{\text{bR}} \mu_{\text{bR}}^0 - \beta p^0 v_{\text{bR}}, \quad (8)$$

where μ_{bR}^0 and p^0 are the chemical potential and the pressure for the pure bR system. The chemical potential and the pressure for the pure bR fluid phase, μ_{f}^0 and p_{f}^0 , were obtained by 2D-Carnahan-Starling like equation of state (2D-CSE)[1, 4], as follows:

$$\beta \mu_{\text{f}}^0 = \ln \left[\frac{\Lambda^2}{v_{\text{bR}}} \right] + \ln [\eta_{\text{bR}}] - \frac{7}{8} \ln [1 - \eta_{\text{bR}}] + \frac{7}{8(1 - \eta_{\text{bR}})} + \frac{9}{8(1 - \eta_{\text{bR}})^2} - 2, \quad (9)$$

$$\beta p_{\text{f}}^0 v_{\text{bR}} = \frac{\eta_{\text{bR}} + \frac{(\eta_{\text{bR}})^2}{8}}{(1 - \eta_{\text{bR}})^2}, \quad (10)$$

where $\Lambda = h(2\pi m_{\text{bR}} k_{\text{B}} T)^{-1/2}$ is the thermal de Broglie wavelength in the 2D space. h and m_{bR} are the Planck constant and the mass for a bR, respectively. The chemical potential and the pressure for the pure bR ordered phase, μ_{ord}^0 and p_{ord}^0 , were obtained by cell theory[4, 38] as follows:

$$\beta \mu_{\text{ord}}^0 = \ln \left[\frac{\Lambda^2}{v_{\text{bR}}} \right] - 2 \ln \left[\frac{\eta_{\text{cp}}}{\eta_{\text{bR}}} - 1 \right] + \frac{2\eta_{\text{cp}}}{\eta_{\text{cp}} - \eta_{\text{bR}}}, \quad (11)$$

$$\beta p_{\text{ord}}^0 v_{\text{bR}} = Z \frac{2\eta_{\text{bR}}}{1 - \frac{\eta_{\text{bR}}}{\eta_{\text{cp}}}}, \quad (12)$$

where $\eta_{\text{cp}} = \pi/(2\sqrt{3}) \approx 0.907$ is the packing fraction at close packing. The first term on the right-hand side, $\ln \left[\frac{\Lambda^2}{v_{\text{bR}}} \right]$, in eq. (9), and eq. (11) does

not affect the phase diagram, because the term is common in the fluid and ordered phases. We adopted the common tangent method to obtain the phase diagrams using free energy curves. The common tangent was drawn on the calculated free energy curves for the fluid and ordered phase.

In our previous study[4], the phase diagrams for the binary hard-disk system were obtained using two-dimensional free volume theory(2D-FVT). The semi-grand potential $\Omega(N_{\text{bR}}, V, T, \mu_{\text{lip}})$ was calculated by 2D-FVT as follows:

$$\Omega(N_{\text{bR}}, V, T, \mu_{\text{lip}}) = F_0(N_{\text{bR}}, V, T) - p^{\text{res}} \langle V_{\text{free}}^{\text{mix}} \rangle_0, \quad (13)$$

where $\langle V_{\text{free}}^{\text{mix}} \rangle_0$ is the free volume for the lipid molecule in a pure bR system. $\langle V_{\text{free}}^{\text{mix}} \rangle_0$ was calculated by 2D-SPT[4, 12]. The equations for F_0 and p^{res} are eq. (8) and eq. (4). The pressure and chemical potential for bR were obtained from $\Omega(N_{\text{bR}}, V, T, \mu_{\text{lip}})$. The phase diagrams were obtained using the following two equations:

$$p_{\text{f}}(\eta_{\text{bR}}^{\text{fluid}}, \eta_{\text{lip}}^{\text{res}}) = p_{\text{ord}}(\eta_{\text{bR}}^{\text{ordered}}, \eta_{\text{lip}}^{\text{res}}), \quad (14)$$

$$\mu_{\text{f,bR}}(\eta_{\text{bR}}^{\text{fluid}}, \eta_{\text{lip}}^{\text{res}}) = \mu_{\text{ord,bR}}(\eta_{\text{bR}}^{\text{ordered}}, \eta_{\text{lip}}^{\text{res}}), \quad (15)$$

where p_{f} and p_{ord} are the pressures for the fluid and ordered phases, $\eta_{\text{bR}}^{\text{fluid}}$ and $\eta_{\text{bR}}^{\text{ordered}}$ are the bR packing fractions for the fluid and ordered phases, $\eta_{\text{lip}}^{\text{res}}$ is the packing fraction of lipid for the reservoir, and $\mu_{\text{f,bR}}$ and $\mu_{\text{ord,bR}}$ are the bR chemical potentials for the fluid and ordered phases.

3. Results

The Helmholtz free energy curves were calculated using the thermodynamic perturbation theory with the effective potential. The phase diagrams were obtained using the common tangent construction on the free energy curves. The phase diagrams for bR monomers (a) and trimers (b) calculated using the AO or the modified AO potentials as the effective potential are shown in FIG. 2.

The coexistence region for the modified AO potential expands at a lower lipid packing fraction than the AO potential. Here, we checked the diagram for the monomers with the lipids (see FIG. 2 (a)). The broadening for the modified AO potential (solid curve) started at about $\eta_{\text{lip}}^{\text{res}} = 0.35$, although that for the AO potential (dashed curve) started at about $\eta_{\text{lip}}^{\text{res}} = 0.7$. We focused on the phase diagrams around $\eta_{\text{lip}}^{\text{res}} = 0.5$ because we estimated the

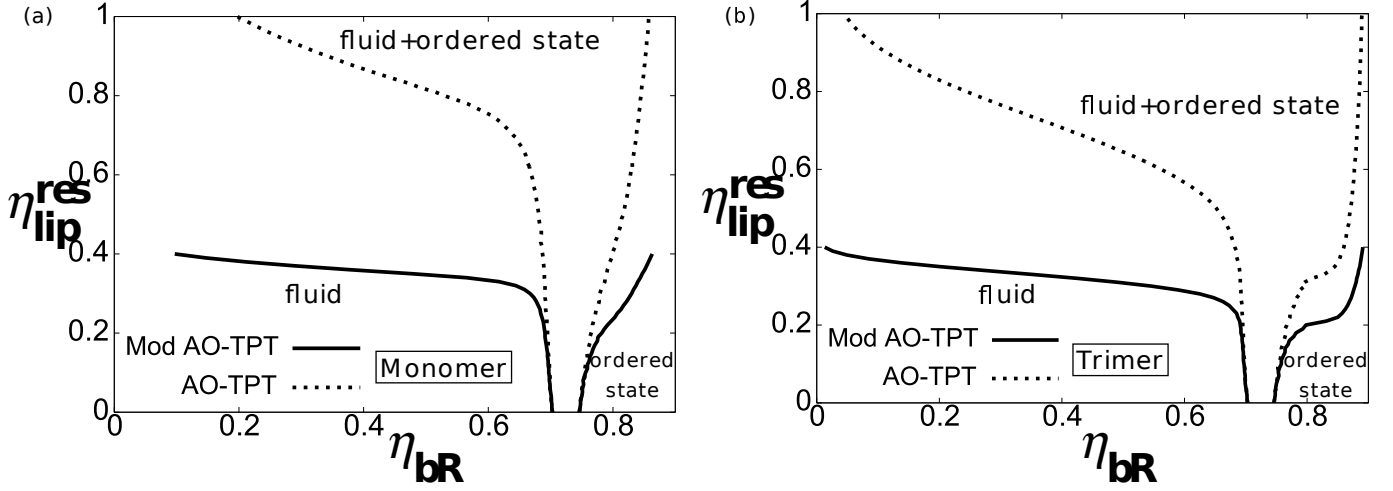


Figure 2: Phase diagrams for (a) bR monomer ($q = 0.16667$) and (b) trimer ($q = 0.08065$). The dotted curves show the phase diagram calculated by the thermodynamic perturbation theory (TPT) with the AO potential. The solid curves show the phase diagram calculated by the thermodynamic perturbation theory with the modified AO potential.

lipid packing fraction of a cell membrane as 0.5 in our previous paper[4]. The broadenings of the coexistence regions for the modified AO potential started lower than $\eta_{\text{lip}}^{\text{res}} = 0.5$. On the other hand, those for the AO potential started higher than $\eta_{\text{lip}}^{\text{res}} = 0.5$ (see FIG. 2 (a) and (b)). Therefore, effective potential dependence is critical.

We defined the critical concentration, $\text{CC}(\eta_{\text{lip}}^{\text{res}})$, as the concentration for the smallest packing fraction for the fluid–ordered phase coexistence state at $\eta_{\text{lip}}^{\text{res}}$. Thus, the $\text{CC}(\eta_{\text{lip}}^{\text{res}})$ gives the boundary curve between the fluid and fluid–ordered states[4]. Unfortunately, we could not obtain the phase diagrams for the modified AO potential systems in the region $\eta_{\text{lip}}^{\text{res}} > 0.4$ [39] (see solid curves in FIG. 2). However, the CC is almost 0 even when $\eta_{\text{lip}}^{\text{res}} = 0.4$. Therefore, we can expect that the CC is very low when $\eta_{\text{lip}}^{\text{res}} = 0.5$. This suggests that the depletion effect can be dominant in the driving force for the bR ordering.

The phase diagrams for the AO potential systems give us a contrasting picture (see dashed curves in FIG. 2). Even when $\eta_{\text{lip}}^{\text{res}} = 0.5$, the CC values were almost similar to those for the pure bR system ($\eta_{\text{lip}}^{\text{res}} = 0.0$). The ratio of CC value at $\eta_{\text{lip}}^{\text{res}} = 0.5$ to that at $\eta_{\text{lip}}^{\text{res}} = 0.0$ is 0.969 in the case of monomer bRs. The ratio for the trimer bRs is 0.927. Therefore, the depletion effect is

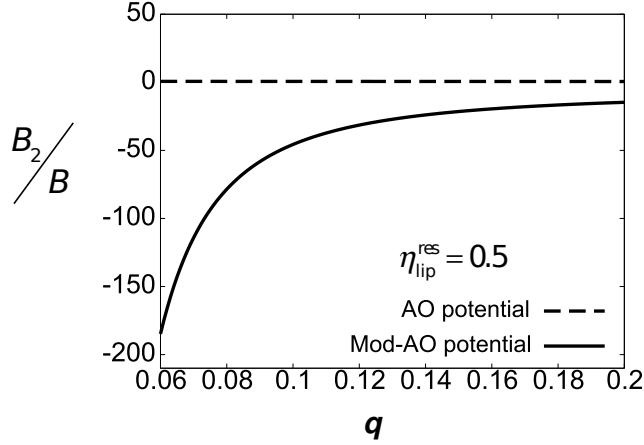


Figure 3: The reduced second virial coefficients B_2/B_2^{HD} at $\eta_{\text{lip}}^{\text{res}} = 0.5$. The dashed and the solid curves show the coefficients for the AO and the modified AO potentials, respectively.

weak in the driving force. We obtained the reduced second virial coefficients B_2/B_2^{HD} (FIG. 3). The coefficients for the modified AO potential were negative, and the absolute value was large when $\eta_{\text{lip}}^{\text{res}} = 0.5$. By contrast, those for the AO potential were positive.

The direct repulsions between bRs and between bR and lipids were the same when we compared the AO potential with the modified AO potential. Then, the difference in the direct interactions is the core repulsion between lipids. Thus, the core repulsions between lipids caused differences in the coefficients (see FIG. 3) and the phase diagrams (see FIG. 2). When the core repulsions between the lipid molecules exist, the calculated results are consistent with the observation of bR crystallization. Therefore, the core repulsion between the lipid molecules is probably one of the essential factors in the discussion of crystallization.

Here, we compared the present study with our previous one[4]. In the previous study, the chemical potentials for the fluid and ordered phases were described using the two-dimensional Carnahan-Starling-like equation of state (2D-CSE) and the two-dimensional free volume theory (2D-FVT) in the case of the pure bR system ($\eta_{\text{lip}}^{\text{res}} = 0$). Thus, the reference systems in both approaches are common. Additionally, we adopted the pressure of the two-dimensional scaled particle theory (2D-SPT) as the reservoir pressure. This

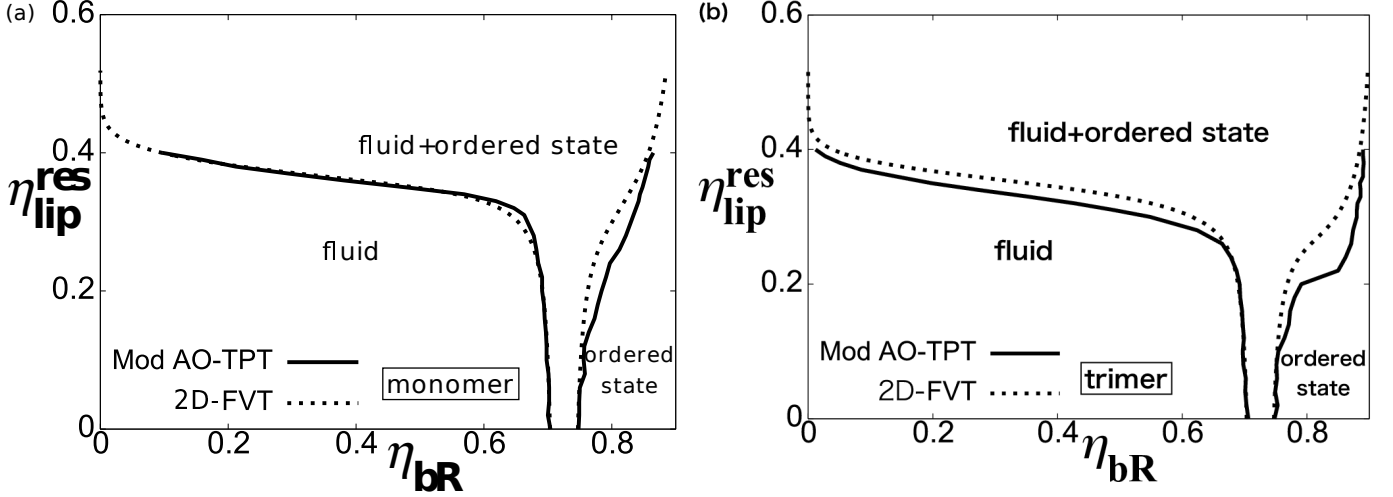


Figure 4: Phase diagrams for (a) bR monomer ($q = 0.16667$) and (b) trimer ($q = 0.08065$). The solid curves show the phase diagrams calculated by the modified AO-TPT approach. The dotted curves show the phase diagrams calculated by the 2D-FVT approach[4].

means that the repulsive cores of the lipids are common. However, the previous study's theoretical framework did not explicitly contain the effective interaction between two bRs[4]. On the other hand, we adopted the modified AO potential as the effective interaction and calculated the phase diagrams using the thermodynamic perturbation theory with the effective interaction (modified AO-TPT) in the present study. The results are compared in FIG. 4.

Because the theories of the reference systems, namely the pure bR system ($\eta_{lip}^{res} = 0$), are common, the coexistence region appears in the same region[40] (see FIG. 4). Even when η_{lip}^{res} increases, the phase diagrams of the previous study are in good agreement with the results given by the present modified AO-TPT study. In particular, the boundaries between the fluid and the fluid-ordered coexistence phases in the present study agree very well with the previous results. The previous research shows that the 2D-FVT approach explains the experimental results semi-quantitatively[4]. Therefore, we can expect that the modified AO-TPT approach is also valid.

On the other hand, we could find a difference between phase diagrams for the bR trimer calculated by modified AO-TPT and 2D-FVT approaches. The coexistence region calculated by the modified AO-TPT approach is slightly wider than that calculated by the 2D-FVT approach. This dif-

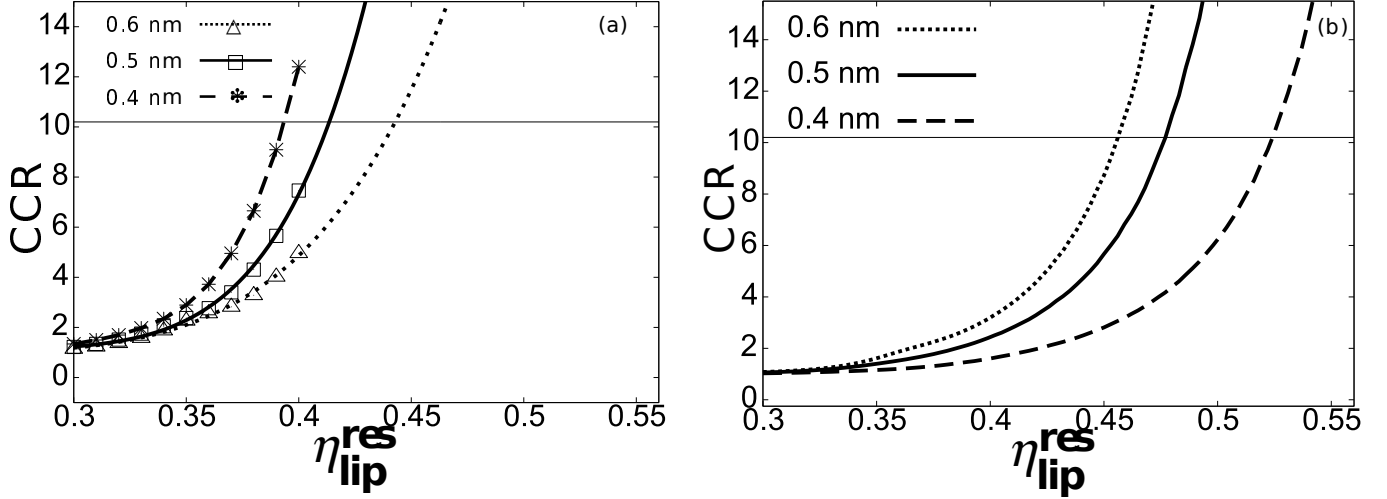


Figure 5: (a) The CCRs were calculated by the modified AO-TPT approach. The triangles, squares, and asterisks show the CCR for $\sigma_{lip} = 0.4, 0.5,$ and $0.6,$ respectively. A dashed line shows the CCR for $\sigma_{lip} = 0.4.$ A solid and dotted lines show the sixth-order polynomial approximation curves of CCR for $\sigma_{lip} = 0.5$ and $0.6,$ respectively. The experimental value of the CCR, $10.2,$ is shown as a thin solid line parallel to the x-axis. (b) The CCRs were calculated by the 2D-FVT approach. The dotted line, a solid line, and a dashed line show the CCR for $\sigma_{lip} = 0.4, 0.5,$ and $0.6,$ respectively[4].

ference increases as the size ratio q approaches 0 (data is not shown). We cannot deny the problem in the modified AO-TPT approach. However, the results of the 2D-FVT approach are more suspicious because the ratio q -dependence on the phase diagram disappears at the small $q.$ This problem of the 2D-FVT approach for small q will be explained later.

The CC for the bR trimer ordering is lower than for the monomer ordering in both theories. For example, when $\eta_{lip}^{res} = 0.4,$ the CCs for bR monomer ordering and trimer ordering calculated by the 2D-FVT approach are 0.100 and $0.042,$ respectively[4]. On the other hand, the CCs for the bR monomer ordering and the trimer ordering calculated by the modified AO-TPT approach are 0.097 and $0.013,$ respectively. The CC for the bR trimer ordering is lower than that for the monomer ordering in each theory. These results correspond to experimental results[28] qualitatively. As with the 2D-FVT approach[4], the modified AO-TPT approach explains the experimental results for bR crystallization[28] qualitatively.

FIG. 5 (a) shows the critical concentration ratios (CCRs) between bR

trimer and monomer obtained from the phase diagrams calculated using the modified AO-TPT approach (symbol). The curves are drawn by sixth-order polynomial approximation when $\sigma_{\text{lip}} = 0.5$ and 0.6 nm. On the other hand, the polynomial approximation for $\sigma_{\text{lip}} = 0.4$ is not drawn because the data are across the line for the CCR=10.2. FIG. 5 (b) has the CCR plots previously calculated by the 2D-FVT approach[4] for comparison. In the present and previous studies[4], the diameter of the lipid molecule is 0.5 nm as a standard. However, this model has arbitrariness. The three lipid diameters $\sigma_{\text{lip}} = 0.4, 0.5,$ and 0.6 nm, were examined to remove the arbitrariness. The experimental value of the CCR, 10.2 , is shown as a solid line parallel to the x -axis. When the CC is too low, we cannot obtain the phase diagram using the TPT approach with the modified AO interaction because the common tangent cannot be drawn on the free energy curves. Therefore, the CCR cannot be calculated up to 10.2 . Thus, the extrapolated plots were drawn when $\sigma_{\text{lip}} = 0.5$ and 0.6 nm. The CCR increases in each theory as $\eta_{\text{lip}}^{\text{res}}$ increases.

The CCRs obtained by the modified AO-TPT approach and the 2D-FVT approach were compared. In the modified AO-TPT approach, the maximum $\eta_{\text{lip}}^{\text{res}}$ where CC can be calculated for all lipid diameters was 0.40 . At $\eta_{\text{lip}}^{\text{res}} = 0.40$, the CCRs obtained by the two approaches were compared. When the σ_{lip} is 0.4 nm, the CCR obtained by the modified AO-TPT approach was 12.4 . On the other hand, the CCR obtained by the 2D-FVT approach was 1.60 . When the σ_{lip} is 0.5 nm, the CCR obtained by the modified AO-TPT approach was 7.46 . On the other hand, the CCR obtained by the 2D-FVT approach was 2.43 . When the σ_{lip} is 0.6 nm, the CCR obtained by the modified AO-TPT approach was 4.96 . On the other hand, the CCR obtained by the 2D-FVT approach was 3.18 . The CCR obtained by the modified AO-TPT approach was larger than that obtained by the 2D-FVT approach for all σ_{lip} . This is because the CC for trimer calculated by the modified AO-TPT approach is smaller than that calculated by the 2D-FVT approach, while the CC for monomer is almost the same between the two theories.

The extrapolated CCR plots obtained by the modified AO-TPT approach agree with experimental CCR value 10.2 at $\eta_{\text{lip}}^{\text{res}} = 0.393, 0.414, 0.443$ for $\sigma_{\text{lip}} = 0.4, 0.5, 0.6$ nm, respectively. $\eta_{\text{lip}}^{\text{res}}$ s correspond to the lipid number densities $3.13, 2.11,$ and $1.57 \times 10^6 \mu\text{m}^{-2}$, respectively. Furthermore, the CCRs obtained by the modified 2D-FVT approach agree with the experimental results at the lipid number density of $4.17, 2.43, 1.61 \times 10^6 \mu\text{m}^{-2}$ for $\sigma_{\text{lip}} = 0.4, 0.5, 0.6$ nm, respectively[4]. On the other hand, the lipid number

density in the single layer of a cell membrane was about $2.5 \times 10^6 \mu m^{-2}$ [36]. Therefore, we expect the CCRs to almost agree with experimental results if we consider the lipid molecule's repulsive core.

The phase diagrams and CCRs for the 2D-FVT and the modified AO-TPT approaches are almost identical. On the other hand, we can find a qualitative difference between their CCRs. Comparing FIG. 5 (a) and (b), the CCRs order of the dependence on the lipid diameter for the modified AO-TPT approach is the inverse of that for the 2D-FVT approach. The CCRs obtained by the 2D-FVT approach increase as the lipid diameter increases. In contrast, the CCRs obtained by the modified AO-TPT approach decrease as the lipid diameter increases. This discrepancy seems to be caused by a problem in the 2D-FVT approach: namely, the calculation of CC for the trimer. García et al. reported that the q -dependence of the phase diagram obtained by the FVT approach disappears in a 3D system as the value q decreases[41]. They further noticed that this result did not agree with an experimental result[41]. This problem in the 3D systems should be conserved in the 2D systems.

We examined the q -dependence using the 2D-FVT approach. FIG. 6 shows the phase diagrams for $q = 0.001$ and 0.0001 calculated using the 2D-FVT approach. These coexistence regions almost overlap each other. This agreement numerically shows that the theoretical approach does not have q dependence when q is small. Thus, we can discuss the relationship between CCR and lipid diameter in the 2D-FVT approach, as follows. The dependence on the lipid diameter for bR monomer CC is more significant than that for bR trimer CC because the value q for monomer CC (about 0.16667) is more significant than that for trimer CC (about 0.08065). Here, the dependence on the lipid diameter is also the q -dependence. Therefore, the CCR dependence mainly obeys the dependence on the lipid diameter for the monomers, and the CCR increases as the lipid diameter increases in the case of the 2D-FVT approach.

The disappearance of the q -dependence for the 2D-FVT approach at small q has to be explained. In the phase diagram calculation, we must find the bR packing fraction for the fluid phase η_{bR}^{fluid} and that for the ordered phase, $\eta_{bR}^{\text{ordered}}$. We obtained them to solve the equations (14) and (15)[4, 12]. The pressure and the chemical potential are expressed by 2D-FVT[4, 12], as

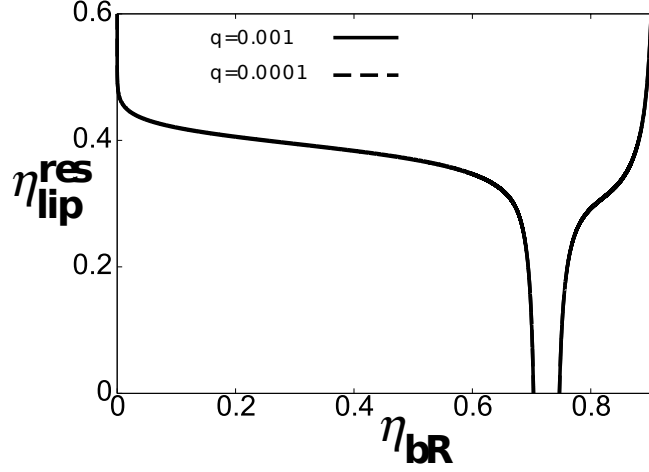


Figure 6: The phase diagrams for small qs calculated by the 2D-FVT approach. The solid and dashed curves show the phase diagrams for $q = 0.001$ and 0.0001 , respectively. These coexistence regions almost overlap each other.

follows:

$$\beta p_f v_{bR} = \beta p_f^0 v_{bR} + \beta p^{\text{res}} v_{bR} \left(\alpha_f - \eta_{bR}^{\text{fluid}} \left(\frac{\partial \alpha_f}{\partial \eta_{bR}^{\text{fluid}}} \right)_{N_{bR}, T, \mu_{\text{lip}}} \right), \quad (16)$$

$$\beta p_{\text{ord}} v_{bR} = \beta p_{\text{ord}}^0 v_{bR} + \beta p^{\text{res}} v_{bR} \left(\alpha_{\text{ord}} - \eta_{bR}^{\text{ordered}} \left(\frac{\partial \alpha_{\text{ord}}}{\partial \eta_{bR}^{\text{ordered}}} \right)_{N_{bR}, T, \mu_{\text{lip}}} \right), \quad (17)$$

$$\beta \mu_{f, bR} = \beta \mu_{f, bR}^0 - \beta p^{\text{res}} v_{bR} \left(\frac{\partial \alpha_f}{\partial \eta_{bR}^{\text{fluid}}} \right)_{V, T, \mu_{\text{lip}}}, \quad (18)$$

$$\beta \mu_{\text{ord}, bR} = \beta \mu_{\text{ord}, bR}^0 - \beta p^{\text{res}} v_{bR} \left(\frac{\partial \alpha_{\text{ord}}}{\partial \eta_{bR}^{\text{ordered}}} \right)_{V, T, \mu_{\text{lip}}}, \quad (19)$$

where, α_f and α_{ord} are the free volume fraction for the fluid phase and ordered phase, respectively. p_f^0 and p_{ord}^0 are the pressure for the fluid and ordered phases in a bR pure system. $\mu_{f, bR}^0$ and $\mu_{\text{ord}, bR}^0$ are the chemical potential for the fluid and ordered phases in the bR pure system. If these values are substituted to the relations (14) and (15), namely $p_f = p_{\text{ord}}$, $\mu_{f, bR} = \mu_{\text{ord}, bR}$,

we obtain two equations, as follows:

$$\beta (p_f^0 - p_{\text{ord}}^0) v_{\text{bR}} + \beta p^{\text{res}} v_{\text{bR}} \left(\alpha_f - \eta_{\text{bR}}^{\text{fluid}} \left(\frac{\partial \alpha_f}{\partial \eta_{\text{bR}}^{\text{fluid}}} \right) - \alpha_{\text{ord}} + \eta_{\text{bR}}^{\text{ordered}} \left(\frac{\partial \alpha_{\text{ord}}}{\partial \eta_{\text{bR}}^{\text{ordered}}} \right) \right) = 0, \quad (20)$$

$$\beta (\mu_{f,\text{bR}}^0 - \mu_{\text{ord},\text{bR}}^0) - \beta p^{\text{res}} v_{\text{bR}} \left(\left(\frac{\partial \alpha_f}{\partial \eta_{\text{bR}}^{\text{fluid}}} \right) - \left(\frac{\partial \alpha_{\text{ord}}}{\partial \eta_{\text{bR}}^{\text{ordered}}} \right) \right) = 0. \quad (21)$$

α_f and α_{ord} are obtained by SPT[4, 12] as follows:

$$\alpha_f = (1 - \eta_{\text{bR}}^{\text{fluid}}) \exp \left[-\frac{2\eta_{\text{bR}}^{\text{fluid}} q}{1 - \eta_{\text{bR}}^{\text{fluid}}} - \frac{\eta_{\text{bR}}^{\text{fluid}} q^2}{(1 - \eta_{\text{bR}}^{\text{fluid}})^2} \right], \quad (22)$$

$$\alpha_{\text{ord}} = (1 - \eta_{\text{bR}}^{\text{ordered}}) \exp \left[-\frac{2\eta_{\text{bR}}^{\text{ordered}} q}{1 - \eta_{\text{bR}}^{\text{ordered}}} - \frac{\eta_{\text{bR}}^{\text{ordered}} q^2}{(1 - \eta_{\text{bR}}^{\text{ordered}})^2} \right]. \quad (23)$$

The partial differentiations are

$$\left(\frac{\partial \alpha_f}{\partial \eta_{\text{bR}}^{\text{fluid}}} \right) = \frac{-(\eta_{\text{bR}}^{\text{fluid}})^2 + (-q^2 + 2q + 2)\eta_{\text{bR}}^{\text{fluid}} - q^2 - 2q - 1}{(1 - \eta_{\text{bR}}^{\text{fluid}})^2} \exp \left[-\frac{2\eta_{\text{bR}}^{\text{fluid}} q}{1 - \eta_{\text{bR}}^{\text{fluid}}} - \frac{\eta_{\text{bR}}^{\text{fluid}} q^2}{(1 - \eta_{\text{bR}}^{\text{fluid}})^2} \right], \quad (24)$$

$$\left(\frac{\partial \alpha_{\text{ord}}}{\partial \eta_{\text{bR}}^{\text{ordered}}} \right) = \frac{-(\eta_{\text{bR}}^{\text{ordered}})^2 + (-q^2 + 2q + 2)\eta_{\text{bR}}^{\text{ordered}} - q^2 - 2q - 1}{(1 - \eta_{\text{bR}}^{\text{ordered}})^2} \exp \left[-\frac{2\eta_{\text{bR}}^{\text{ordered}} q}{1 - \eta_{\text{bR}}^{\text{ordered}}} - \frac{\eta_{\text{bR}}^{\text{ordered}} q^2}{(1 - \eta_{\text{bR}}^{\text{ordered}})^2} \right]. \quad (25)$$

The pressure in the reservoir is expressed using SPT[4, 12]: namely, eq. (4). Then, $\beta p^{\text{res}} v_{\text{bR}}$ is expressed using $\eta_{\text{lip}}^{\text{res}}$ as, follows:

$$\beta p^{\text{res}} v_{\text{bR}} = \frac{\eta_{\text{lip}}^{\text{res}} q^{-2}}{(1 - \eta_{\text{lip}}^{\text{res}})^2}. \quad (26)$$

The first term on the left-hand side in eqs. (20) and (21) does not depend on q . On the other hand, we must confirm the behavior of the second term

on the left-hand side in eq. (20) at the limit of $q = 0$ because the part $\beta p^{\text{res}} v_{\text{bR}}$ goes to infinity, and the remaining part—namely, the part in the parentheses—goes to zero. The second term on the left-hand side in eq. (21) also has a similar problem. Thus, these second terms are expanded to polynomials to discuss the q -dependence.

The left-hand sides of eqs. (20) and (21) are expanded to the polynomial functions of q , as follows[42].

$$(p_{\text{f}}^0 - p_{\text{ord}}^0) v_{\text{bR}} + \frac{\eta_{\text{lip}}^{\text{res}}}{(1 - \eta_{\text{lip}}^{\text{res}})^2} \left(\frac{-(\eta_{\text{bR}}^{\text{fluid}})^2}{(1 - \eta_{\text{bR}}^{\text{fluid}})^2} + \frac{(\eta_{\text{bR}}^{\text{ordered}})^2}{(1 - \eta_{\text{bR}}^{\text{ordered}})^2} \right) + O(q) = 0 \quad (27)$$

$$\begin{aligned} & \mu_{\text{f}}^0 - \mu_{\text{ord}}^0 + \\ & \frac{\eta_{\text{lip}}^{\text{res}}}{(1 - \eta_{\text{lip}}^{\text{res}})^2} \left(\frac{1 - 4\eta_{\text{bR}}^{\text{fluid}} + 2(\eta_{\text{bR}}^{\text{fluid}})^2}{(1 - \eta_{\text{bR}}^{\text{fluid}})^2} - \frac{1 - 4\eta_{\text{bR}}^{\text{ordered}} + 2(\eta_{\text{bR}}^{\text{ordered}})^2}{(1 - \eta_{\text{bR}}^{\text{ordered}})^2} \right) \\ & + O(q) = 0 \end{aligned} \quad (28)$$

These limit equations gave us a phase diagram that almost overlapped those in FIG. 6. The q -dependence disappears at the limit of $q = 0$. Therefore, the phase diagram of the 2D-FVT approach does not depend on q for small q .

This disappearance of the q -dependence originates in α_{f} and α_{ord} . The same theory, namely SPT, is used to express both α_{f} and α_{ord} . Therefore, the 0th-order terms of q for the fluid and ordered phases cancel each other in eqs. (27) and (28). In the 3D system, a similar problem has been pointed out, and the geometrical consideration for α_{ord} was proposed instead of SPT[41, 43].

4. CONCLUSION

The phase diagrams of binary hard-disk systems were calculated to discuss the driving force of bR crystallization. To study the effects of the core repulsive force between lipid molecules as depletants, we calculated the phase diagram and CCR using the thermodynamic perturbation theory with two effective interactions between bRs[24, 25, 34]. The current approach was entirely different from the previous study based on simple theories [4]. However, the results agreed with the experimental ones only when we considered

the core repulsive force between lipid molecules. Despite the different calculation methods, the results were the same as the previous one. Therefore, the present results also support that the core repulsion between lipid molecules plays an essential role in the driving force of crystallization. In the future, we think that verification by simulation should be necessary.

5. Acknowledgments

This work was also supported by Japan Society for the Promotion of Science (JSPS) KAKENHI Grant Nos. JP22K03558 and JP21K18604, JP19H01863, JP19K03772, and JP22J13118. The computation was performed using Research Center for Computational Science, Okazaki, Japan (Project: 22-IMS-C101 and 22-IMS-C113) and the Research Institute for Information Technology, Kyushu University.

References

- [1] R. Henderson, P. N. T. Unwin, *Nature* 257 (1975) 28, <https://doi.org/10.1038/257028a0>.
- [2] R. Henderson, J. M. Baldwin, T. A. Ceska, F. Zemlin, E. Beckmann, K. H. Downing, *J. Mol. Biol.* 213 (1990) 899, [https://doi.org/10.1016/S0022-2836\(05\)80271-2](https://doi.org/10.1016/S0022-2836(05)80271-2).
- [3] M. P. Krebs, T. A. Isenbarger, *Biochim. Biophys. Acta* 1460 (2000) 15, [https://doi.org/10.1016/S0005-2728\(00\)00126-2](https://doi.org/10.1016/S0005-2728(00)00126-2).
- [4] K. Suda, A. Suematsu, R. Akiyama, *J. Chem. Phys.* 154 (2021) 204904, <https://doi.org/10.1063/5.0044399>.
- [5] S. Asakura, F. Oosawa, *J. Chem. Phys.* 22 (1954) 1255, <https://doi.org/10.1063/1.1740347>.
- [6] S. Asakura, F. Oosawa, *J. Pol. Sci.* 33 (1958) 183, <https://doi.org/10.1002/pol.1958.1203312618>.
- [7] R. Roth, B. Götzelmann, S. Dietrich, *Phys. Rev. Lett.* 83 (1999) 448, <https://doi.org/10.1103/PhysRevLett.83.448>.
- [8] Y. Rosenfeld, *Phys. Rev. Lett.* 63 (1989) 980, <https://doi.org/10.1103/PhysRevLett.63.980>.

- [9] R. Roth, R. Evans, A. Lang, G. Kahl, *J. Phys.: Condens. Matter* 14 (2002) 12063,
<https://doi.org/10.1088/0953-8984/14/46/313>.
- [10] Y. Nakamura, S. Arai, M. Kinoshita, A. Yoshimori, R. Akiyama, *J. Chem. Phys.* 151 (2019) 044506,
<https://doi.org/10.1063/1.5100040>.
- [11] A. Vrij, *Pure Appl. Chem.* 48 (1976) 471,
<https://doi.org/10.1351/pac197648040471>.
- [12] H. N. W. Lekkerkerker, R. Tuinier, *Colloids and the Depletion Interaction*, Springer, New York, 2011,
<https://doi.org/10.1007/978-94-007-1223-2>.
- [13] H. N. W. Lekkerkerker, W. C. K. Poon, P. N. Pusey, A. Stroobants, P. B. Warren, *Europhys. Lett.* 20 (1992) 559,
<https://doi.org/10.1209/0295-5075/20/6/015>.
- [14] D. Frenkel, A. A. Louis, *Phys. Rev. Lett.* 68 (1992) 3363,
<https://doi.org/10.1103/PhysRevLett.68.3363>.
- [15] M. Dijkstra, D. Frenkel, J. P. Hansen, *J. Chem. Phys.* 101 (1994) 3179,
<https://doi.org/10.1063/1.468468>.
- [16] M. Dijkstra, D. Frenkel, *Phys. Rev. Lett.* 72 (1994) 298,
<https://doi.org/10.1103/PhysRevLett.72.298>.
- [17] M. Dijkstra and R. van Roij and R. Evans, *Phys. Rev. Lett.* 81 (1998) 2268,
<https://doi.org/10.1103/PhysRevLett.81.2268>.
- [18] M. Dijkstra and R. van Roij and R. Evans, *Phys. Rev. Lett.* 82 (1999) 117,
<https://doi.org/10.1103/PhysRevLett.82.117>.
- [19] M. Dijkstra and R. van Roij and R. Evans, *Phys. Rev. E* 59 (1999) 5744,
<https://doi.org/10.1103/PhysRevE.59.5744>.
- [20] M. Dijkstra, J. M. Brader, R. Evans, *J. Phys.: Condens. Matter* 11 (1999) 10079,
<https://doi.org/10.1088/0953-8984/11/50/304>.

- [21] M. Dijkstra and R. van Roij and R. Roth and A. Fortini, *Phys. Rev. E* 73 (2006) 041404,
<https://doi.org/10.1103/PhysRevE.73.041404>.
- [22] G. Cinacchi, Y. Martínez-Ratón, L. Mederos, G. Navascués, A. Tani, E. Velasco, *J. Chem. Phys.* 127 (2007) 214501,
<https://doi.org/10.1063/1.2804330>.
- [23] E. López-Sánchez, C. D. Estrada-Álvarez, G. Pérez-Ángel, J. M. Méndez-Alcaraz, P. González-Mozuelos, R. Castañeda-Priego, *J. Chem. Phys.* 139 (2013) 104908,
<https://doi.org/10.1063/1.4820559>.
- [24] E. Velasco, G. Navascués, L. Mederos, *Phys. Rev. E* 60 (1999) 3158,
<https://doi.org/10.1103/PhysRevE.60.3158>.
- [25] A. Suematsu, A. Yoshimori, R. Akiyama, *Europhys. Lett.* 116 (2016) 38004,
<https://doi.org/10.1209/0295-5075/116/38004>.
- [26] A. M. Tom, W. K. Kim, C. Hyeon, *J. Chem. Phys.* 154 (2021) 214901,
<https://doi.org/10.1063/5.0048554>.
- [27] M. P. Krebs, W. Li, T. P. Halambek, *J. Mol. Biol.* 267 (1997) 172,
<https://doi.org/10.1006/jmbi.1996.0848>.
- [28] T. A. Isenbarger, M. P. Krebs, *Biochemistry* 38 (1999) 9023,
<https://doi.org/10.1021/bi9905563>.
- [29] J. T. Lee, M. Robert, *Phys. Rev. E* 60 (1999) 7198,
<https://doi.org/10.1103/PhysRevE.60.7198>.
- [30] J. Russo, N. B. Wilding, *Phys. Rev. Lett.* 119 (2017) 115702,
<https://doi.org/10.1103/PhysRevLett.119.115702>.
- [31] S.-C. Lin, M. Oettel, *Phys. Rev. E* 98 (2018) 012608,
<https://doi.org/10.1103/PhysRevE.98.012608>.
- [32] H. Reiss, H. L. Frisch, J. L. Lebowitz, *J. Chem. Phys.* 31 (1959) 369,
<https://doi.org/10.1063/1.1730361>.

- [33] E. Helfand, H. L. Frisch, J. L. Lebowitz, *J. Chem. Phys.* 34 (1961) 1037, <https://doi.org/10.1063/1.1731629>.
- [34] Y. Tamura, A. Yoshimori, A. Suematsu, R. Akiyama, *Europhys. Lett* 129 (2020) 66001, <https://doi.org/10.1209/0295-5075/129/66001>.
- [35] A. Rakovich, A. Sukhanova, N. Bouchonville, E. Lukashev, V. Oleinikov, M. Artemyev, V. Lesnyak, N. Gaponik, M. Molinari, M. Troyon, Y. P. Rakovich, J. F. Donegan, I. Nabiev, *Nano Lett.* 10 (2010) 2640, <https://doi.org/10.1021/nl1013772>.
- [36] B. Alberts, A. Johnson, J. Lewis, D. Morgan, M. Raff, K. Roberts, P. Walter, *Molecular Biology of THE CELL*, Garland Science, New York, 2015.
- [37] E. P. Bernard, W. Krauth, *Phys. Rev. Lett.* 107 (2011) 155704, <https://doi.org/10.1103/PhysRevLett.107.155704>.
- [38] Z. W. Salsburg, W. W. Wood, *J. Chem. Phys.* 37 (1962) 798, <https://doi.org/10.1063/1.1733163>.
- [39] The phase diagram cannot be calculated by modified AO–TPT approach when the CC is very low because the common tangent cannot be drawn on the free energy.
- [40] The coexistence regions are $\eta_{bR} = 0.703 - 0.747$ (2D–FVT approach) and $\eta_{bR} = 0.703 - 0.746$ (TPT approach). There is slight difference because the calculation methods are different.
- [41] Á. G. García, J. Opdam, R. Tuinier, M. Vis, *Chem. Phys. Lett.* 709 (2018) 16, <https://doi.org/10.1016/j.cplett.2018.08.028>.
- [42] See the supplementary material for the derivation.
- [43] J. Opdam, M. P. M. Schelling, R. Tuinier, *J. chem. Phys.* 154 (2021) 074902, <https://doi.org/10.1063/5.0037963>.

Supplementary Material for Two-Dimensional Ordering of Bacteriorhodopsins in a Lipid Bilayer and Effects Caused by Repulsive Core between Lipid Molecules on Lateral Depletion Interaction: A Study based on a Thermodynamic Perturbation Theory

The chemical potential for bR and the pressure in the fluid and ordered phases, $\mu_{f,bR}$, $\mu_{ord,bR}$, p_f , and p_{ord} are obtained by 2D-FVT as follows:

$$\beta\mu_{f,bR} = \beta\mu_{f,bR}^0 - \beta p^{\text{res}} v_{bR} \left(\frac{\partial\alpha_f}{\partial\eta_{bR}^{\text{fluid}}} \right)_{V,T,\mu_{lip}}, \quad (29)$$

$$\beta\mu_{ord,bR} = \beta\mu_{ord,bR}^0 - \beta p^{\text{res}} v_{bR} \left(\frac{\partial\alpha_{ord}}{\partial\eta_{bR}^{\text{ordered}}} \right)_{V,T,\mu_{lip}}, \quad (30)$$

$$\beta p_f v_{bR} = \beta p_f^0 v_{bR} + \beta p^{\text{res}} v_{bR} \left(\alpha_f - \eta_{bR}^{\text{fluid}} \left(\frac{\partial\alpha_f}{\partial\eta_{bR}^{\text{fluid}}} \right)_{N_{bR},T,\mu_{lip}} \right), \quad (31)$$

$$\beta p_{ord} v_{bR} = \beta p_{ord}^0 v_{bR} + \beta p^{\text{res}} v_{bR} \left(\alpha_{ord} - \eta_{bR}^{\text{ordered}} \left(\frac{\partial\alpha_{ord}}{\partial\eta_{bR}^{\text{ordered}}} \right)_{N_{bR},T,\mu_{lip}} \right), \quad (32)$$

where β is the inverse temperature, μ_f^0 and μ_{ord}^0 are the chemical potential for the bR pure system in the fluid and ordered phases, p_f^0 and p_{ord}^0 are the pressure for the bR pure system in the fluid and ordered phases, v_{bR} is the area of one bR, p^{res} is the pressure in the reservoir, α_f and α_{ord} are the free volume fraction in the fluid and ordered phases, and η_{bR}^{fluid} and $\eta_{bR}^{\text{ordered}}$ are the packing fraction of bRs in the fluid and ordered phases. The phase diagrams were obtained by 2D-FVT approach in the previous study[4] solving the following two equations:

$$\beta (\mu_{f,bR}^0 - \mu_{ord,bR}^0) - \beta p^{\text{res}} v_{bR} \left(\left(\frac{\partial\alpha_f}{\partial\eta_{bR}^{\text{fluid}}} \right) - \left(\frac{\partial\alpha_{ord}}{\partial\eta_{bR}^{\text{ordered}}} \right) \right) = 0, \quad (33)$$

$$\beta (p_f^0 - p_{ord}^0) v_{bR} + \beta p^{\text{res}} v_{bR} \left(\alpha_f - \eta_{bR}^{\text{fluid}} \left(\frac{\partial\alpha_f}{\partial\eta_{bR}^{\text{fluid}}} \right) - \alpha_{ord} + \eta_{bR}^{\text{ordered}} \left(\frac{\partial\alpha_{ord}}{\partial\eta_{bR}^{\text{ordered}}} \right) \right) = 0. \quad (34)$$

μ_f^0 , μ_{ord}^0 , p_f^0 , and p_{ord}^0 are independent of q . The pressure for the reservoir, p^{res} , are calculated by SPT[4, 12] as follows:

$$\beta p^{\text{res}} v_{\text{bR}} = \frac{\eta_{\text{lip}}^{\text{res}} q^{-2}}{(1 - \eta_{\text{lip}}^{\text{res}})^2}. \quad (35)$$

α for the fluid and ordered phases are calculated by SPT[4, 12] as follows:

$$\alpha_f = (1 - \eta_{\text{bR}}^{\text{fluid}}) \exp \left[-\frac{2\eta_{\text{bR}}^{\text{fluid}} q}{1 - \eta_{\text{bR}}^{\text{fluid}}} - \frac{\eta_{\text{bR}}^{\text{fluid}} q^2}{(1 - \eta_{\text{bR}}^{\text{fluid}})^2} \right], \quad (36)$$

$$\alpha_{\text{ord}} = (1 - \eta_{\text{bR}}^{\text{ordered}}) \exp \left[-\frac{2\eta_{\text{bR}}^{\text{ordered}} q}{1 - \eta_{\text{bR}}^{\text{ordered}}} - \frac{\eta_{\text{bR}}^{\text{ordered}} q^2}{(1 - \eta_{\text{bR}}^{\text{ordered}})^2} \right]. \quad (37)$$

The partial differentiations of α for the fluid and ordered phases are as follows:

$$\left(\frac{\partial \alpha_f}{\partial \eta_{\text{bR}}^{\text{fluid}}} \right) = \frac{-(\eta_{\text{bR}}^{\text{fluid}})^2 + (-q^2 + 2q + 2)\eta_{\text{bR}}^{\text{fluid}} - q^2 - 2q - 1}{(1 - \eta_{\text{bR}}^{\text{fluid}})^2} \exp \left[-\frac{2\eta_{\text{bR}}^{\text{fluid}} q}{1 - \eta_{\text{bR}}^{\text{fluid}}} - \frac{\eta_{\text{bR}}^{\text{fluid}} q^2}{(1 - \eta_{\text{bR}}^{\text{fluid}})^2} \right], \quad (38)$$

$$\left(\frac{\partial \alpha_{\text{ord}}}{\partial \eta_{\text{bR}}^{\text{ordered}}} \right) = \frac{-(\eta_{\text{bR}}^{\text{ordered}})^2 + (-q^2 + 2q + 2)\eta_{\text{bR}}^{\text{ordered}} - q^2 - 2q - 1}{(1 - \eta_{\text{bR}}^{\text{ordered}})^2} \exp \left[-\frac{2\eta_{\text{bR}}^{\text{ordered}} q}{1 - \eta_{\text{bR}}^{\text{ordered}}} - \frac{\eta_{\text{bR}}^{\text{ordered}} q^2}{(1 - \eta_{\text{bR}}^{\text{ordered}})^2} \right]. \quad (39)$$

To examine the convergence of the equations (33) and (34) at the limit of $q = 0$, α and $\left(\frac{\partial \alpha}{\partial \eta_{\text{bR}}} \right)$ are expanded to polynomial functions of q . The Maclaurin expansions of α_f and α_{ord} are written as follows:

$$\alpha_f(q) = \alpha_f(0) + \left(\frac{\partial \alpha_f}{\partial q} \right)_{q=0} \cdot q + \frac{1}{2} \left(\frac{\partial^2 \alpha_f}{\partial q^2} \right)_{q=0} \cdot q^2 + O(q^3), \quad (40)$$

$$\alpha_{\text{ord}}(q) = \alpha_{\text{ord}}(0) + \left(\frac{\partial \alpha_{\text{ord}}}{\partial q} \right)_{q=0} \cdot q + \frac{1}{2} \left(\frac{\partial^2 \alpha_{\text{ord}}}{\partial q^2} \right)_{q=0} \cdot q^2 + O(q^3). \quad (41)$$

$\alpha(0)$ for the fluid and ordered phases are as follows:

$$\alpha_f(0) = 1 - \eta_{\text{bR}}^{\text{fluid}}, \quad (42)$$

$$\alpha_{\text{ord}}(0) = 1 - \eta_{\text{bR}}^{\text{ordered}}. \quad (43)$$

$\left(\frac{\partial\alpha}{\partial q}\right)$ for the fluid and ordered phases are as follows:

$$\left(\frac{\partial\alpha_f}{\partial q}\right) = \left(-2\eta_{\text{bR}}^{\text{fluid}} - \frac{2\eta_{\text{bR}}^{\text{fluid}}q}{(1 - \eta_{\text{bR}}^{\text{fluid}})}\right) \exp\left[\frac{-2\eta_{\text{bR}}^{\text{fluid}}q}{1 - \eta_{\text{bR}}^{\text{fluid}}} - \frac{\eta_{\text{bR}}^{\text{fluid}}q^2}{(1 - \eta_{\text{bR}}^{\text{fluid}})^2}\right], \quad (44)$$

$$\left(\frac{\partial\alpha_{\text{ord}}}{\partial q}\right) = \left(-2\eta_{\text{bR}}^{\text{ordered}} - \frac{2\eta_{\text{bR}}^{\text{ordered}}q}{(1 - \eta_{\text{bR}}^{\text{ordered}})}\right) \exp\left[\frac{-2\eta_{\text{bR}}^{\text{ordered}}q}{1 - \eta_{\text{bR}}^{\text{ordered}}} - \frac{\eta_{\text{bR}}^{\text{ordered}}q^2}{(1 - \eta_{\text{bR}}^{\text{ordered}})^2}\right]. \quad (45)$$

$\left(\frac{\partial\alpha}{\partial q}\right)_{q=0}$ for the fluid and ordered phases are as follows:

$$\left(\frac{\partial\alpha_f}{\partial q}\right)_{q=0} = -2\eta_{\text{bR}}^{\text{fluid}}, \quad (46)$$

$$\left(\frac{\partial\alpha_{\text{ord}}}{\partial q}\right)_{q=0} = -2\eta_{\text{bR}}^{\text{ordered}}. \quad (47)$$

$\left(\frac{\partial^2\alpha}{\partial q^2}\right)$ for the fluid and ordered phases are as follows:

$$\left(\frac{\partial^2\alpha_f}{\partial q^2}\right) = (1 - \eta_{\text{bR}}^{\text{fluid}}) \left(\frac{-2\eta_{\text{bR}}^{\text{fluid}}}{(1 - \eta_{\text{bR}}^{\text{fluid}})^2} + \left(\frac{-2\eta_{\text{bR}}^{\text{fluid}}}{1 - \eta_{\text{bR}}^{\text{fluid}}} - \frac{2\eta_{\text{bR}}^{\text{fluid}}q}{(1 - \eta_{\text{bR}}^{\text{fluid}})^2}\right)^2\right) \exp\left[\frac{-2\eta_{\text{bR}}^{\text{fluid}}q}{1 - \eta_{\text{bR}}^{\text{fluid}}} - \frac{\eta_{\text{bR}}^{\text{fluid}}q^2}{(1 - \eta_{\text{bR}}^{\text{fluid}})^2}\right], \quad (48)$$

$$\left(\frac{\partial^2\alpha_{\text{ord}}}{\partial q^2}\right) = (1 - \eta_{\text{bR}}^{\text{ordered}}) \left(\frac{-2\eta_{\text{bR}}^{\text{ordered}}}{(1 - \eta_{\text{bR}}^{\text{ordered}})^2} + \left(\frac{-2\eta_{\text{bR}}^{\text{ordered}}}{1 - \eta_{\text{bR}}^{\text{ordered}}} - \frac{2\eta_{\text{bR}}^{\text{ordered}}q}{(1 - \eta_{\text{bR}}^{\text{ordered}})^2}\right)^2\right) \exp\left[\frac{-2\eta_{\text{bR}}^{\text{ordered}}q}{1 - \eta_{\text{bR}}^{\text{ordered}}} - \frac{\eta_{\text{bR}}^{\text{ordered}}q^2}{(1 - \eta_{\text{bR}}^{\text{ordered}})^2}\right]. \quad (49)$$

$\left(\frac{\partial^2\alpha}{\partial q^2}\right)_{q=0}$ for the fluid and ordered phases are as follows:

$$\left(\frac{\partial^2\alpha_f}{\partial q^2}\right)_{q=0} = \frac{-2\eta_{\text{bR}}^{\text{fluid}}}{1 - \eta_{\text{bR}}^{\text{fluid}}} + \frac{4(\eta_{\text{bR}}^{\text{fluid}})^2}{1 - \eta_{\text{bR}}^{\text{fluid}}}, \quad (50)$$

$$\left(\frac{\partial^2\alpha_{\text{ord}}}{\partial q^2}\right)_{q=0} = \frac{-2\eta_{\text{bR}}^{\text{ordered}}}{1 - \eta_{\text{bR}}^{\text{ordered}}} + \frac{4(\eta_{\text{bR}}^{\text{ordered}})^2}{1 - \eta_{\text{bR}}^{\text{ordered}}}. \quad (51)$$

The results of the Maclaurin expansions of α for the fluid and ordered phases are as follows:

$$\alpha_f(q) = (1 - \eta_{bR}^{\text{fluid}}) - 2\eta_{bR}^{\text{fluid}}q + \left(\frac{-\eta_{bR}^{\text{fluid}} + 2(\eta_{bR}^{\text{fluid}})^2}{1 - \eta_{bR}^{\text{fluid}}} \right) q^2 + O(q^3), \quad (52)$$

$$\alpha_{\text{ord}}(q) = (1 - \eta_{bR}^{\text{ordered}}) - 2\eta_{bR}^{\text{ordered}}q + \left(\frac{-\eta_{bR}^{\text{ordered}} + 2(\eta_{bR}^{\text{ordered}})^2}{1 - \eta_{bR}^{\text{ordered}}} \right) q^2 + O(q^3). \quad (53)$$

We define $\left(\frac{\partial \alpha}{\partial \eta_{bR}} \right)$ as $G(q)$ for simple expression. The Maclaurin expansions of $G(q)$ for the fluid and ordered phases are as follows:

$$G_f(q) = G_f(0) + \left(\frac{\partial G_f}{\partial q} \right)_{q=0} \cdot q + \frac{1}{2} \left(\frac{\partial^2 G_f}{\partial q^2} \right)_{q=0} \cdot q^2 + O(q^3), \quad (54)$$

$$G_{\text{ord}}(q) = G_{\text{ord}}(0) + \left(\frac{\partial G_{\text{ord}}}{\partial q} \right)_{q=0} \cdot q + \frac{1}{2} \left(\frac{\partial^2 G_{\text{ord}}}{\partial q^2} \right)_{q=0} \cdot q^2 + O(q^3) \quad (55)$$

We define $f(q)$ and $e(q)$ as follows:

$$f(q) \equiv \frac{-\eta_{bR}^2 + (-q^2 + 2q + 2)\eta_{bR} - q^2 - 2q - 1}{(1 - \eta_{bR})^2}, \quad (56)$$

$$e(q) \equiv \exp \left[-\frac{2\eta_{bR}q}{1 - \eta_{bR}} - \frac{\eta_{bR}q^2}{(1 - \eta_{bR})^2} \right], \quad (57)$$

$$G(q) = f(q) \cdot e(q). \quad (58)$$

$G(0)$ for the fluid and ordered phases are -1 . $\left(\frac{\partial G}{\partial q} \right)$ for the fluid and ordered phases are as follows:

$$\left(\frac{\partial G_f}{\partial q} \right) = \left(\frac{\partial f_f}{\partial q} \right) \cdot e_f(q) + f_f(q) \cdot \left(\frac{\partial e_f}{\partial q} \right), \quad (59)$$

$$\left(\frac{\partial G_{\text{ord}}}{\partial q} \right) = \left(\frac{\partial f_{\text{ord}}}{\partial q} \right) \cdot e_{\text{ord}}(q) + f_{\text{ord}}(q) \cdot \left(\frac{\partial e_{\text{ord}}}{\partial q} \right). \quad (60)$$

$\left(\frac{\partial f}{\partial q} \right)$ for the fluid and ordered phases are as follows:

$$\left(\frac{\partial f_f}{\partial q} \right) = \frac{(-2q + 2)\eta_{bR}^{\text{fluid}} - 2q - 2}{(1 - \eta_{bR}^{\text{fluid}})^2}, \quad (61)$$

$$\left(\frac{\partial f_{\text{ord}}}{\partial q} \right) = \frac{(-2q + 2)\eta_{bR}^{\text{ordered}} - 2q - 2}{(1 - \eta_{bR}^{\text{ordered}})^2}. \quad (62)$$

$\left(\frac{\partial e}{\partial q}\right)$ for the fluid and ordered phases are as follows:

$$\left(\frac{\partial e_f}{\partial q}\right) = \left(-\frac{2\eta_{\text{bR}}^{\text{fluid}}}{1-\eta_{\text{bR}}^{\text{fluid}}} - \frac{2\eta_{\text{bR}}^{\text{fluid}} q}{(1-\eta_{\text{bR}}^{\text{fluid}})^2}\right) \exp\left[-\frac{2\eta_{\text{bR}}^{\text{fluid}} q}{1-\eta_{\text{bR}}^{\text{fluid}}} - \frac{\eta_{\text{bR}}^{\text{fluid}} q^2}{(1-\eta_{\text{bR}}^{\text{fluid}})^2}\right], \quad (63)$$

$$\left(\frac{\partial e_{\text{ord}}}{\partial q}\right) = \left(-\frac{2\eta_{\text{bR}}^{\text{ordered}}}{1-\eta_{\text{bR}}^{\text{ordered}}} - \frac{2\eta_{\text{bR}}^{\text{ordered}} q}{(1-\eta_{\text{bR}}^{\text{ordered}})^2}\right) \exp\left[-\frac{2\eta_{\text{bR}}^{\text{ordered}} q}{1-\eta_{\text{bR}}^{\text{ordered}}} - \frac{\eta_{\text{bR}}^{\text{ordered}} q^2}{(1-\eta_{\text{bR}}^{\text{ordered}})^2}\right]. \quad (64)$$

$\left(\frac{\partial G}{\partial q}\right)_{q=0}$ for the fluid and ordered phases are as follows:

$$\left(\frac{\partial G_f}{\partial q}\right)_{q=0} = -\frac{2}{1-\eta_{\text{bR}}^{\text{fluid}}} \cdot 1 - 1 \cdot \left(-\frac{2\eta_{\text{bR}}^{\text{fluid}}}{1-\eta_{\text{bR}}^{\text{fluid}}}\right) = -2, \quad (65)$$

$$\left(\frac{\partial G_{\text{ord}}}{\partial q}\right)_{q=0} = -\frac{2}{1-\eta_{\text{bR}}^{\text{ordered}}} \cdot 1 - 1 \cdot \left(-\frac{2\eta_{\text{bR}}^{\text{ordered}}}{1-\eta_{\text{bR}}^{\text{ordered}}}\right) = -2. \quad (66)$$

$\left(\frac{\partial^2 G}{\partial q^2}\right)$ for the fluid and ordered phases are as follows:

$$\left(\frac{\partial^2 G_f}{\partial q^2}\right) = \left(\frac{\partial^2 f_f}{\partial q^2}\right) \cdot e_f(q) + 2 \left(\frac{\partial f_f}{\partial q}\right) \cdot \left(\frac{\partial e_f}{\partial q}\right) + f_f(q) \cdot \left(\frac{\partial^2 e_f}{\partial q^2}\right), \quad (67)$$

$$\left(\frac{\partial^2 G_{\text{ord}}}{\partial q^2}\right) = \left(\frac{\partial^2 f_{\text{ord}}}{\partial q^2}\right) \cdot e_{\text{ord}}(q) + 2 \left(\frac{\partial f_{\text{ord}}}{\partial q}\right) \cdot \left(\frac{\partial e_{\text{ord}}}{\partial q}\right) + f_{\text{ord}}(q) \cdot \left(\frac{\partial^2 e_{\text{ord}}}{\partial q^2}\right). \quad (68)$$

$\left(\frac{\partial^2 f}{\partial q^2}\right)$ for the fluid and ordered phases are as follows:

$$\left(\frac{\partial^2 f_f}{\partial q^2}\right) = \frac{-2\eta_{\text{bR}}^{\text{fluid}} - 2}{(1-\eta_{\text{bR}}^{\text{fluid}})^2}, \quad (69)$$

$$\left(\frac{\partial^2 f_{\text{ord}}}{\partial q^2}\right) = \frac{-2\eta_{\text{bR}}^{\text{ordered}} - 2}{(1-\eta_{\text{bR}}^{\text{ordered}})^2}. \quad (70)$$

$\left(\frac{\partial^2 e}{\partial q^2}\right)$ for the fluid and ordered phases are as follows:

$$\begin{aligned} \left(\frac{\partial^2 e_f}{\partial q^2}\right) &= \left(\frac{-2\eta_{\text{bR}}^{\text{fluid}}}{(1-\eta_{\text{bR}}^{\text{fluid}})^2} + \left(-\frac{2\eta_{\text{bR}}^{\text{fluid}}}{1-\eta_{\text{bR}}^{\text{fluid}}} - \frac{2\eta_{\text{bR}}^{\text{fluid}} q}{(1-\eta_{\text{bR}}^{\text{fluid}})^2}\right)^2\right) \\ &\exp\left[-\frac{2\eta_{\text{bR}}^{\text{fluid}} q}{1-\eta_{\text{bR}}^{\text{fluid}}} - \frac{\eta_{\text{bR}}^{\text{fluid}} q^2}{(1-\eta_{\text{bR}}^{\text{fluid}})^2}\right], \end{aligned} \quad (71)$$

$$\begin{aligned} \left(\frac{\partial^2 e_{\text{ord}}}{\partial q^2} \right) &= \left(\frac{-2\eta_{\text{bR}}^{\text{ordered}}}{(1 - \eta_{\text{bR}}^{\text{ordered}})^2} + \left(-\frac{2\eta_{\text{bR}}^{\text{ordered}}}{1 - \eta_{\text{bR}}^{\text{ordered}}} - \frac{2\eta_{\text{bR}}^{\text{ordered}} q}{(1 - \eta_{\text{bR}}^{\text{ordered}})^2} \right)^2 \right) \\ &\exp \left[-\frac{2\eta_{\text{bR}}^{\text{ordered}} q}{1 - \eta_{\text{bR}}^{\text{ordered}}} - \frac{\eta_{\text{bR}}^{\text{ordered}} q^2}{(1 - \eta_{\text{bR}}^{\text{ordered}})^2} \right]. \end{aligned} \quad (72)$$

$\left(\frac{\partial^2 G}{\partial q^2} \right)_{q=0}$ for the fluid and ordered phases are as follows:

$$\begin{aligned} \left(\frac{\partial^2 G_{\text{f}}}{\partial q^2} \right)_{q=0} &= \frac{-2\eta_{\text{bR}}^{\text{fluid}} - 2}{(1 - \eta_{\text{bR}}^{\text{fluid}})^2} + 2 \left(\frac{-2}{(1 - \eta_{\text{bR}}^{\text{fluid}})} \cdot \frac{-2\eta_{\text{bR}}^{\text{fluid}}}{(1 - \eta_{\text{bR}}^{\text{fluid}})} \right) + -1 \cdot \frac{-2\eta_{\text{bR}}^{\text{fluid}} + 4(\eta_{\text{bR}}^{\text{fluid}})^2}{(1 - \eta_{\text{bR}}^{\text{fluid}})^2} \\ &= \frac{-2 + 8\eta_{\text{bR}}^{\text{fluid}} - 4(\eta_{\text{bR}}^{\text{fluid}})^2}{(1 - \eta_{\text{bR}}^{\text{fluid}})^2}, \end{aligned} \quad (73)$$

$$\begin{aligned} \left(\frac{\partial^2 G_{\text{ord}}}{\partial q^2} \right)_{q=0} &= \frac{-2\eta_{\text{bR}}^{\text{ordered}} - 2}{(1 - \eta_{\text{bR}}^{\text{ordered}})^2} + 2 \left(\frac{-2}{(1 - \eta_{\text{bR}}^{\text{ordered}})} \cdot \frac{-2\eta_{\text{bR}}^{\text{ordered}}}{(1 - \eta_{\text{bR}}^{\text{ordered}})} \right) + \\ &-1 \cdot \frac{-2\eta_{\text{bR}}^{\text{ordered}} + 4(\eta_{\text{bR}}^{\text{ordered}})^2}{(1 - \eta_{\text{bR}}^{\text{ordered}})^2} \\ &= \frac{-2 + 8\eta_{\text{bR}}^{\text{ordered}} - 4(\eta_{\text{bR}}^{\text{ordered}})^2}{(1 - \eta_{\text{bR}}^{\text{ordered}})^2}. \end{aligned} \quad (74)$$

The results of the Maclaurin expansions of $G(q)$ for the fluid and ordered phases are as follows

$$G_{\text{f}}(q) = -1 - 2q + \frac{-1 + 4\eta_{\text{bR}}^{\text{fluid}} - 2(\eta_{\text{bR}}^{\text{fluid}})^2}{(1 - \eta_{\text{bR}}^{\text{fluid}})^2} q^2 + O(q^3), \quad (75)$$

$$G_{\text{ord}}(q) = -1 - 2q + \frac{-1 + 4\eta_{\text{bR}}^{\text{ordered}} - 2(\eta_{\text{bR}}^{\text{ordered}})^2}{(1 - \eta_{\text{bR}}^{\text{ordered}})^2} q^2 + O(q^3). \quad (76)$$

The $\alpha - \eta_{\text{bR}} \left(\frac{\partial \alpha}{\partial \eta_{\text{bR}}} \right)$ for the fluid and ordered phases are as follows:

$$\alpha_{\text{f}} - \eta_{\text{bR}}^{\text{fluid}} \left(\frac{\partial \alpha_{\text{f}}}{\partial \eta_{\text{bR}}^{\text{fluid}}} \right) = 1 - \frac{(\eta_{\text{bR}}^{\text{fluid}})^2}{(1 - \eta_{\text{bR}}^{\text{fluid}})^2} q^2 + O(q^3), \quad (77)$$

$$\alpha_{\text{ord}} - \eta_{\text{bR}}^{\text{ordered}} \left(\frac{\partial \alpha_{\text{ord}}}{\partial \eta_{\text{bR}}^{\text{ordered}}} \right) = 1 - \frac{(\eta_{\text{bR}}^{\text{ordered}})^2}{(1 - \eta_{\text{bR}}^{\text{ordered}})^2} q^2 + O(q^3). \quad (78)$$

Substituting the eqs. (35), (75), and (76) to (33), the eq (33) is calculated as

$$\mu_f^0 - \mu_{\text{ord}}^0 + \frac{\eta_{\text{lip}}^{\text{res}}}{(1 - \eta_{\text{lip}}^{\text{res}})^2} \cdot \left(\frac{1 - 4\eta_{\text{bR}}^{\text{fluid}} + 2(\eta_{\text{bR}}^{\text{fluid}})^2}{(1 - \eta_{\text{bR}}^{\text{fluid}})^2} - \frac{1 - 4\eta_{\text{bR}}^{\text{ordered}} + 2(\eta_{\text{bR}}^{\text{ordered}})^2}{(1 - \eta_{\text{bR}}^{\text{ordered}})^2} \right) + O(q) = 0. \quad (79)$$

Substituting the eqs. (35), (77), and (78) to (34), the eq (34) is calculated as

$$(p_f^0 - p_{\text{ord}}^0) v_{\text{bR}} + \frac{\eta_{\text{lip}}^{\text{res}}}{(1 - \eta_{\text{lip}}^{\text{res}})^2} \cdot \left(\frac{-(\eta_{\text{bR}}^{\text{fluid}})^2}{(1 - \eta_{\text{bR}}^{\text{fluid}})^2} + \frac{(\eta_{\text{bR}}^{\text{ordered}})^2}{(1 - \eta_{\text{bR}}^{\text{ordered}})^2} \right) + O(q) = 0 \quad . \quad (80)$$

The eqs. (79) and (80) show that the solutions of eqs. (33) and (34) are independent of q at the limit of $q = 0$. The phase diagram was obtained using the equations (79) and (80). The coexistence region of this phase diagram almost overlap that of phase diagrams at very small q , $q = 0.001$ and $q = 0.0001$ (data is not shown).